Electronic Supplementary Material (ESI) for Journal of Materials Chemistry B.

SUPPORTING INFORMATION

Plasmon Induced Dual Excited Synergistic Effect in Au/Metal-Organic Frameworks Composite for Enhanced Antibacterial Therapy

Qiuyang Xu,[1†] Xuewwei Liao,[1†] Wenchao Hu,[1] Wenyuan Liu,[1] Chen Wang*[1,2]

[1]Key Laboratory of Drug Quality Control and Pharmacovigilance, Ministry of Education, China Pharmaceutical University, Nanjing 211198, China

[2]School of Chemistry and Materials Science, Nanjing Normal University, Nanjing 210023, China

*To whom correspondence should be addressed. E-mail: wangchen@cpu.edu.cn; wangchen@njnu.edu.cn

MATERIALS AND METHODS

Reagents

Zinc nitrate hexahydrate ($Zn(NO_3)_2 \cdot 6H_2O$) was purchased from Xilong Scientific Co., Ltd. Guangdong, China. Sodium borohydride ($NaBH_4$), polyvinylpyrrolidone (PVP), pyrazine, 1,3-Diphenylisobenzofuran (DPBF) and 3,3′,5,5′-tetramethylbenzidine (TMB) were purchased from Sigma-Aldrich. Tetrakis (4-carboxyphenyl) porphyrin (H_2TCPP) was purchased from HEOWNS, Tianjin, China. Sodium citrate was purchased from Sinopharm Chemical Reagent Co., Ltd. Tetrachloroauric acid ($HAuCl_4 \cdot 4H_2O$) was purchased from the First Reagent Factory (Shanghai, China). Singlet oxygen sensor green (SOSG) was purchased from Meilunbio Co., Ltd. 2,2,6,6-Tetramethyl-4-piperidone (4-oxo-TMP) and tetrabutylammonium hexafluorophosphate ($TBAPF_6$) were purchased from Shanghai Aladdin Biochemical Technology Co., Ltd. (Shanghai, China). All reagents were of analytical grade. All solutions were prepared using ultrapure water (18.2 MΩ cm^{-1}).

Instruments

UV-vis adsorption spectroscopic characterization was performed using UV-3600 Plus Spectrophotometer (SHIMAZU, Japan). The morphologies of each sample were characterized by transmission electron microscope (TEM, JEM-2100, Japan) and scanning electron microscope (SEM, S-4800, Japan). X-ray diffraction (XRD) patterns were determined by D8 Advance X-ray diffractometer (Bruker, Germany) equipped with Cu Kα (λ =1.54 Å) radiation in the 2θ range of 5-50° at a low scanning speed of 0.2° per minute. X-ray photoelectron Spectroscopy (XPS) spectra were analyzed by PHI 5000 VersaProbe (Japan). The binding energy was calibrated by means of the C1s peak energy (284.8 eV). EPR spectra were obtained by Bruker EMXplus electron paramagnetic resonance spectrometer at room temperature. Zeta potentials were obtained by Malvern Zetasizer Nano ZS90. Fluorescence spectra were measured on a fluorescence spectrophotometer (HORIBA, FluoroMax-4). Fluorescence images and dark field images were acquired on an Olympus RTS-2 fluorescence inverted microscope equipped with dark field condenser and colored CCD. All electrochemical measurements were recorded by CHI 660E instrument (Chenhua, China).

Fabrication of Zn-MOFs nanosheets

The Zn-MOFs nanosheets were synthesized according to a reported procedure.[1] Briefly, $Zn(NO_3)_2 \cdot 6H_2O$ (8.9 mg, 0.03 mmol), pyrazine (0.8 mg, 0.01 mmol) and PVP (20 mg) were dissolved in DMF/ethanol mixture solution (12 mL, v/v=3:1). Then, H_2TCPP (4.0 mg,0.005 mmol) in DMF/ethanol mixture solution (4 mL, v/v=3:1) was added drop wisely to the solution mentioned above. After that, the mixed solution was ultrasonicated for 10 min and kept at 353 K for 4 h. The light purple solid products were washed by ethanol for three times and collected by centrifuging at 8,000 r.p.m. for 10 min.

Fabrication of Au nanostars (AuNSs)

AuNSs were synthesized following a previous work.[2] First, the gold seeds (15 nm) were first prepared using the classic Frens method. The 0.1 g/mL PVP aqueous solution was added into the as-prepared gold colloidal (15 nm) solution under stirring for 24 h. Then, the obtained PVP-stabilized particles were centrifuged to remove the dissolved PVP and re-dispersed in anhydrous ethanol. Afterwards, 110 μL tetrachloroauric acid (25 mM) aqueous solution was added into 10 mL PVP (10 mM) solution, followed by rapid addition of PVP-coated gold particles (2 mL) under continuous stirring until the solution color changed from pink to blue.

Fabrication of AuNSs modified Zn-MOFs (AuNSs/Zn-MOFs)

Zn-MOFs nanosheets were assembled with AuNSs through electrostatic interaction. 1 mg Zn-MOFs was re-dispersed in 2 mL ultrapure water. The AuNSs/Zn-MOFs hybrid was prepared by mixing both the AuNSs and Zn-MOFs solutions with a volume ratio of 2:1. Then, the mixture was sonicated for more than 1 h and the resulting sample was obtained.

The ROS generation ability of AuNSs/Zn-MOFs

For the oxidation of TMB, 50 μL 5 mg/mL TMB solution and 50 μL AuNSs/Zn-MOFs were added into 2mL HAc/NaAc buffer solution. Then, the mixture was irradiated under a 660 nm laser (150 mW) for various time periods. The increased absorption band of TMB_{ox} at 652 nm was measured to determine the generation of ROS. For the degradation of DPBF, 20 μL 2.5mg/mL DPBF/DMF solution and 50 μL

AuNSs/Zn-MOFs were added into 2mL DMF. Then, the mixture was irradiated under a 660 nm laser (150 mW) for various time periods. The decreased absorption band of DPBF at 415 nm was measured to determine the generation of singlet oxygen ($^1O_2$). Singlet oxygen sensor green (SOSG) is a fluorescent probe with highly selective for $^1O_2$. 50 μL 10 μM SOSG and 50 μL AuNSs/Zn-MOFs were added into 2 mL 10 % D_2O. The SOSG fluorescence spectroscopy was recorded with the excitation at 488 nm after the laser irradiation.

Dark-field scattering spectroscopy

The ITO slides were pre-treated by ultrasonic cleaning with acetone, ethanol and water for 3 times, respectively, and then blow-dried with N_2. Afterwards, the cleaned ITO slides were immersed into AuNSs and AuNSs/Zn-MOFs hybrid solution for immobilization (1 h) and then blow-dried with N_2. The AuNSs were imaged under a dark-field microscope and the dark-field scattering spectrum of single particle was collected.

Electrochemical characterization

The open-circuit photovoltage decay (OCPVD) were measured using OCP-time tests with light off and on. Mott-Schottky plots were derived from impedance-potential tests conducted at a frequency of 1000 Hz with light off and on. Electrochemical impedance spectroscopy was recorded under open circuit (amplitude for 5 mV and frequency ranging from 10^6 to 0.1 Hz). Cyclic voltammetry was recorded with three electrode system and deoxygenated $TBAPF_6$ acetonitrile solution (0.1 M) was supporting electrolyte. A nitrogen atmosphere was maintained during the measurement.

Bacterial culture

The monoclonal of *E. coli* and *S. aureus* bacteria on the solid LB agar medium was transferred to liquid LB medium and cultured at 37 °C under 175 rpm, respectively. Controlling the bacterial growth density to just reach the logarithmic growth period.

Antibacterial activity assay

T0he antibacterial experiment was divided into four groups: bacteria + PBS, bacteria + AuNSs, bacteria + Zn-MOFs and bacteria + AuNSs/Zn-MOFs. For the growth-inhibition experiment, the groups were exposed to 660 nm (150 mW) light

irradiation for various period. The bacterial suspensions were collected after further incubation for 12 h (37 °C under 175 rpm). For the plate-counting experiment, the bacterial suspensions were irradiated for 1.0 h and then diluted 1000 times. 20 μL diluted bacterial suspensions were spread on solid LB agar medium and cultured at 37 °C for 12 h. Bacterial suspensions in different groups were irradiated with 660 nm laser. Subsequently, all bacterial were treated with AO and PI in PBS for 15 min in the dark condition and then visualized using fluorescence inverted microscope.

Preparation of bacterial samples for SEM

All treated bacteria were washed with PBS for 3 times. Glutaraldehyde (2.5 %) was used for fixing the bacterial cells at 4 °C for overnight. Then, the cells were washed using PBS and dehydrated by methanol.

EXPERIMENTAL DATA

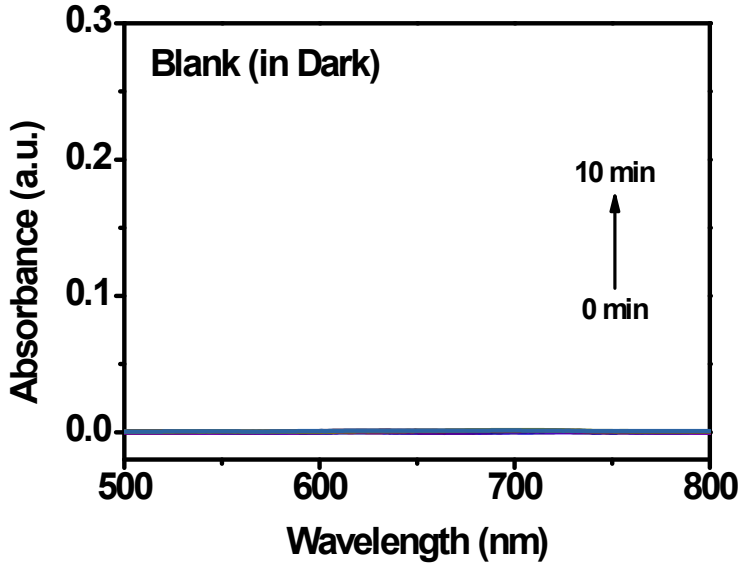

Figure S1. The UV-vis spectra of TMB oxidation product in blank control group for various time (in dark condition).

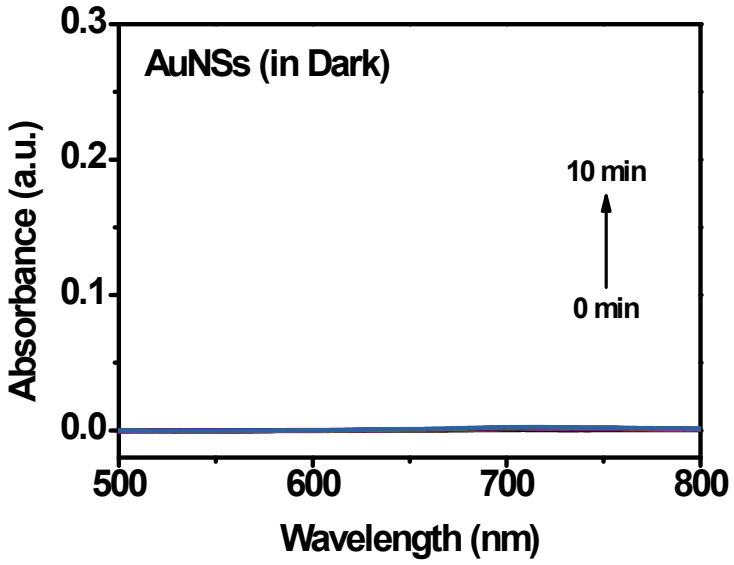

Figure S2. The UV-vis spectra of TMB oxidation product in AuNSs for various time (in dark condition).

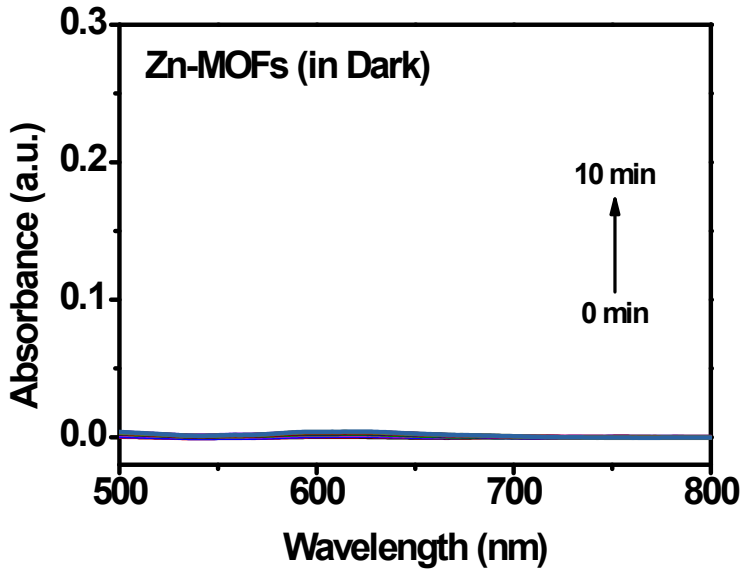

Figure S3. The UV-vis spectra of TMB oxidation product in Zn-MOFs for various time (in dark condition).

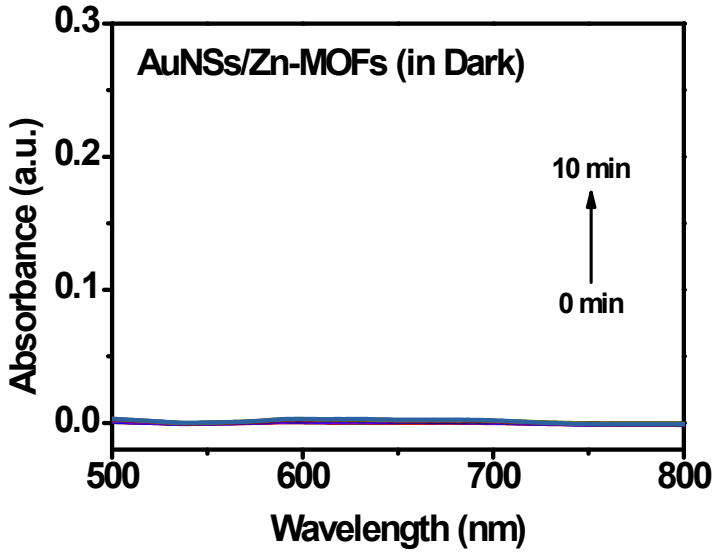

Figure S4. The UV-vis spectra of TMB oxidation product in AuNSs/Zn-MOFs hybrid for various time (in dark condition).

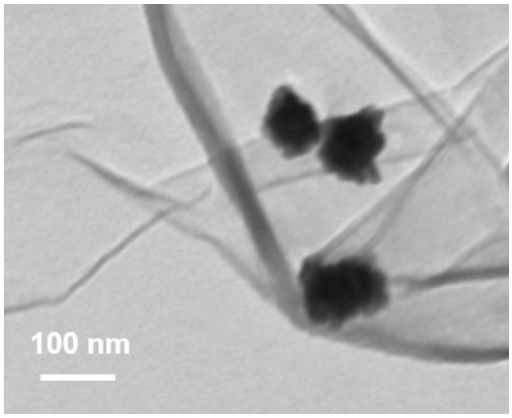

Figure S5. TEM image of AuNSs/Zn-MOFs hybrid after 10 min light irradiation.

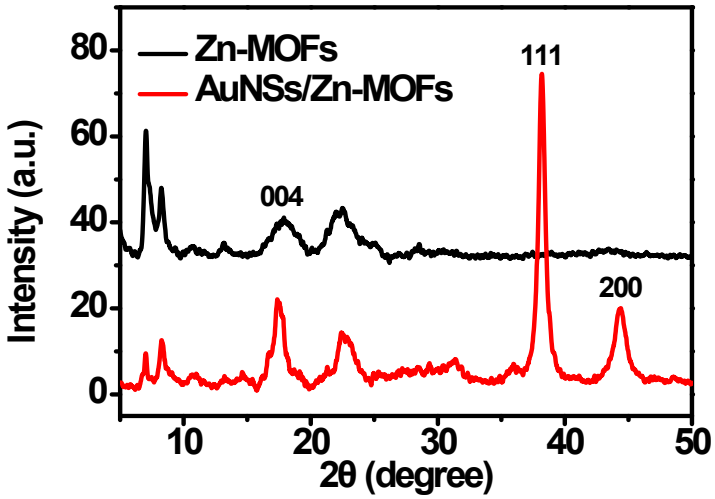

Figure S6. XRD patterns of Zn-MOFs and AuNSs/Zn-MOFs after 10 min light irradiation.

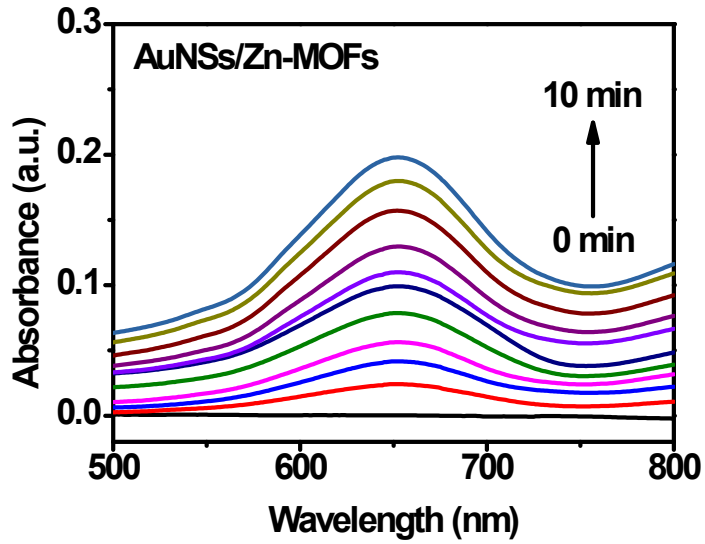

Figure S7. The UV-vis spectra of TMB oxidation product in the AuNSs/Zn-MOFs hybrid under light irradiation for various time.

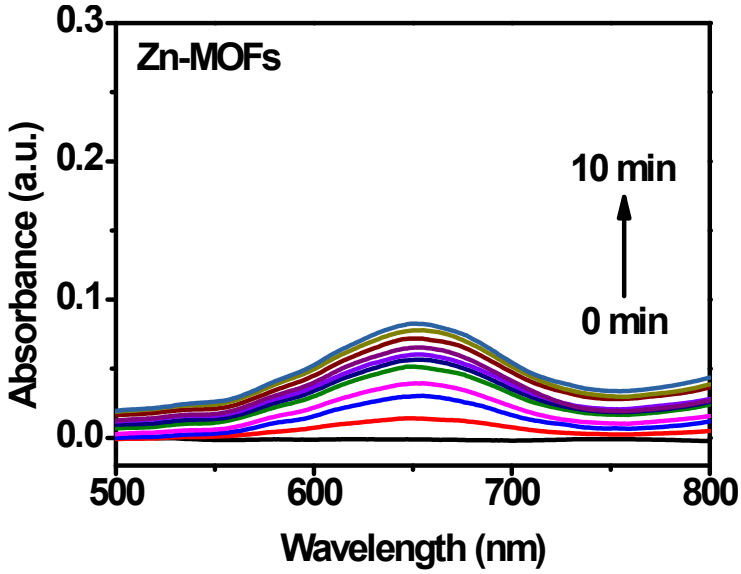

Figure S8. The UV-vis spectra of TMB oxidation product in Zn-MOFs under light irradiation for various time.

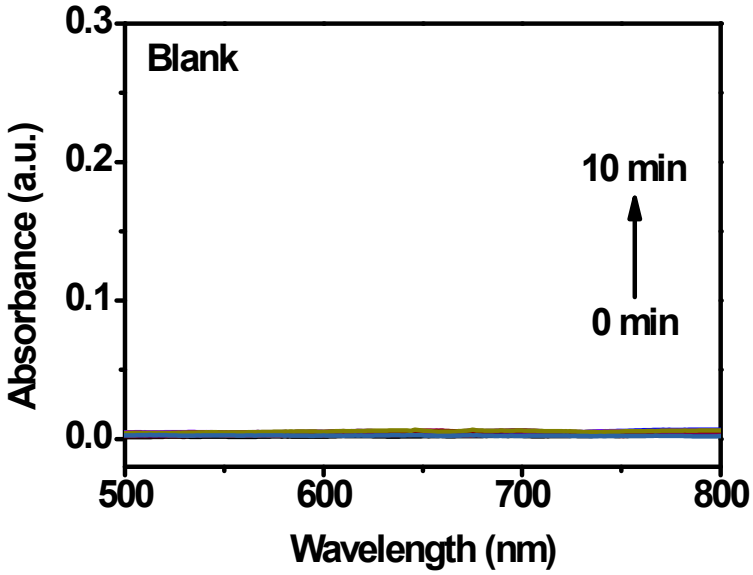

Figure S9. The UV-vis spectra of TMB oxidation product in the blank group under light irradiation for various time.

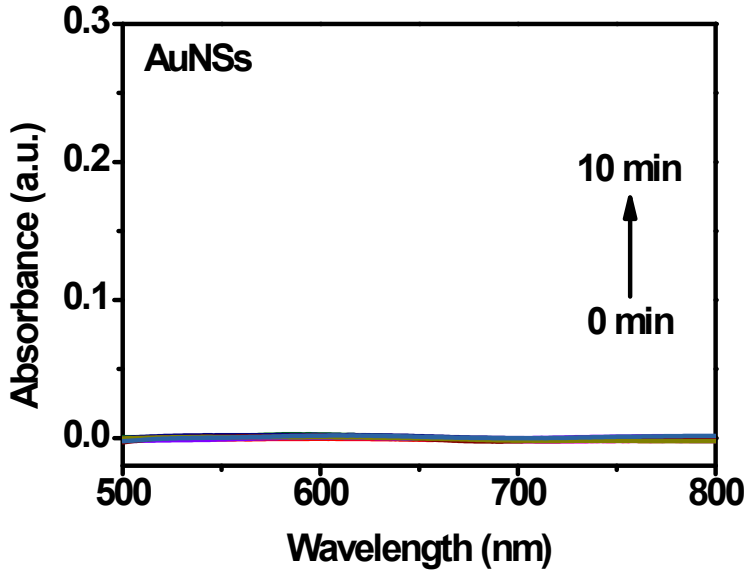

Figure S10. The UV-vis spectra of TMB oxidation product in the AuNSs under light irradiation for various time.

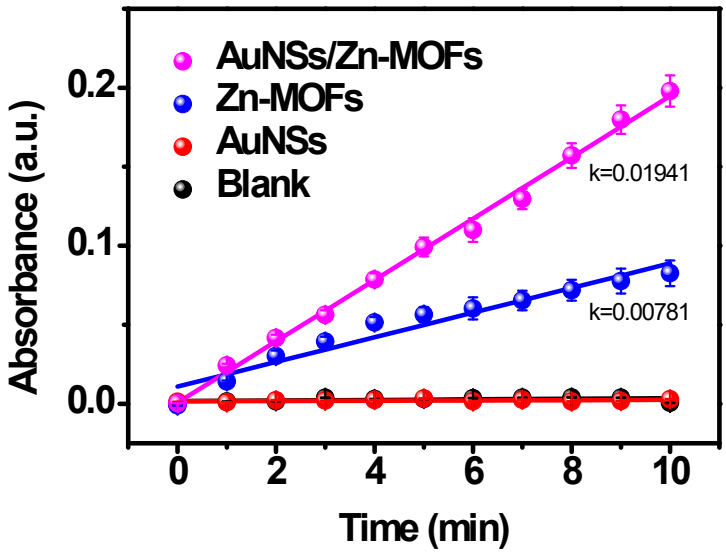

Figure S11. UV-vis peak intensity for the TMB oxidation product vs light irradiation time in the blank, AuNSs, Zn-MOFs and AuNSs/Zn-MOFs hybrid.

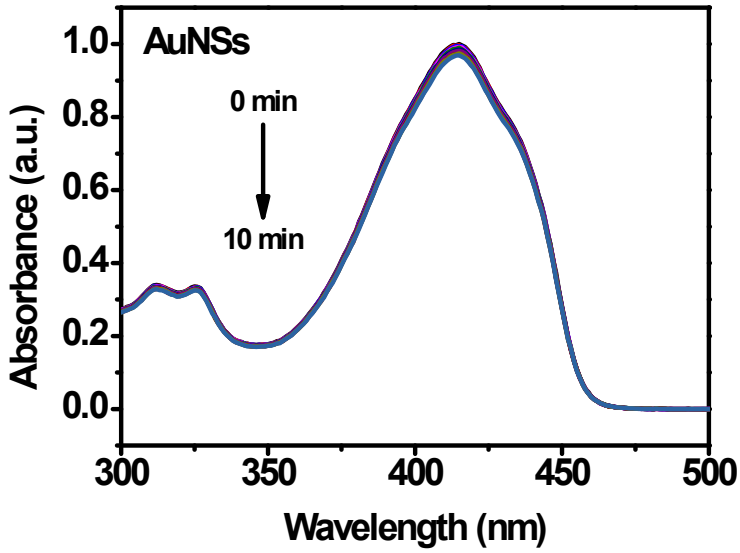

Figure S12. The UV-vis spectra of DPBF in the AuNSs under light irradiation for various time.

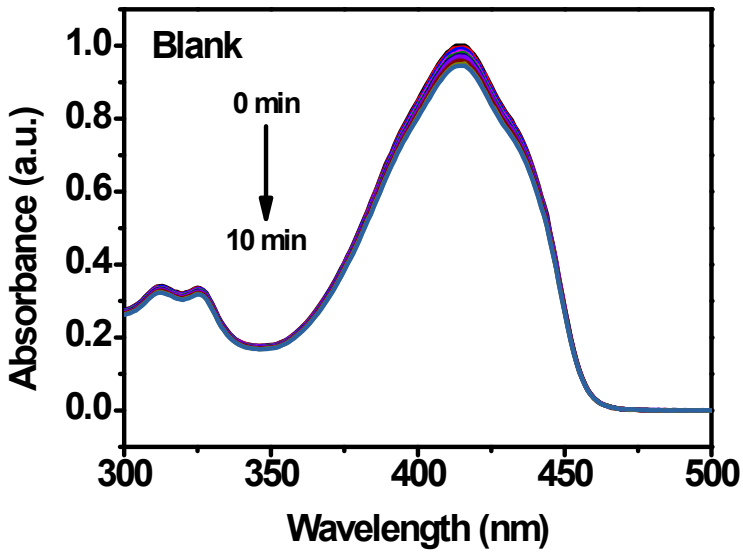

Figure S13. The UV-vis spectra of DPBF in the blank group under light irradiation for various time.

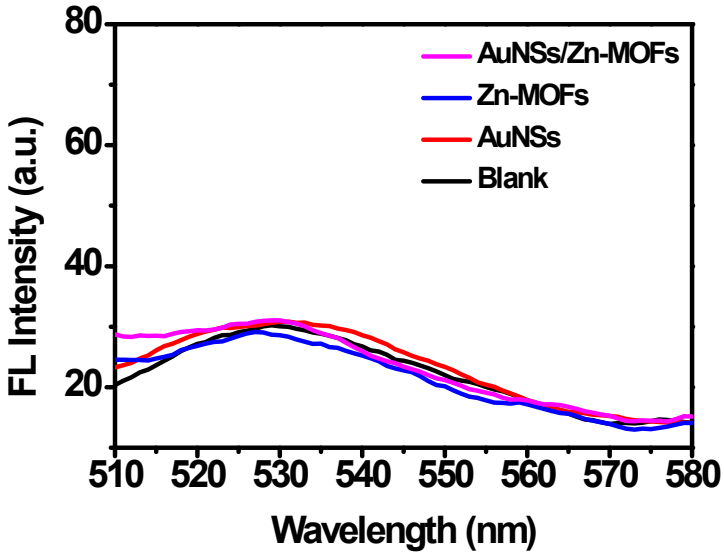

Figure S14. Fluorescence spectra of SOSG in the blank, AuNSs, Zn-MOFs and AuNSs/Zn-MOFs hybrid without light irradiation.

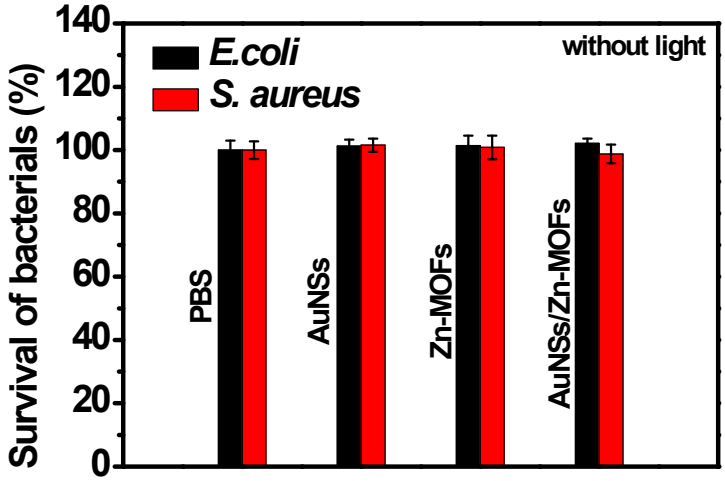

Figure S15. *S. aureus* and *E. coli* incubated in LB medium with different groups for 24h in the absence of irradiation.

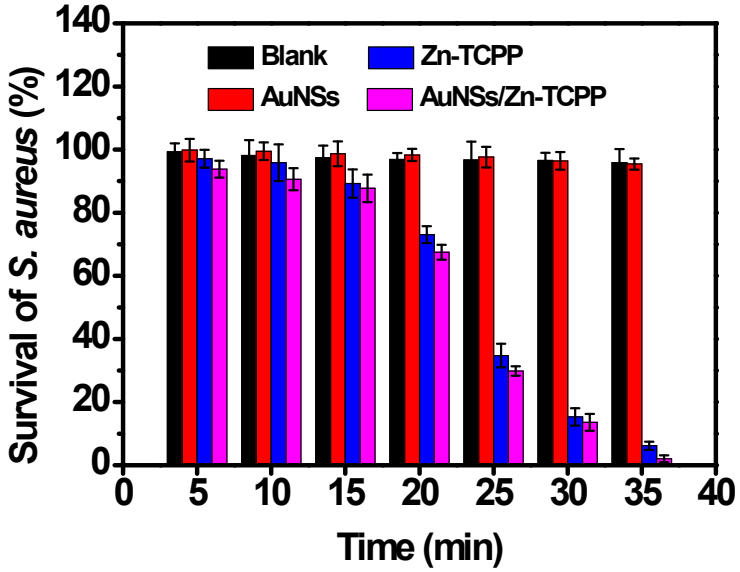

Figure S16. The antibacterial activities of *S. aureus* in different groups upon laser irradiation for various times.

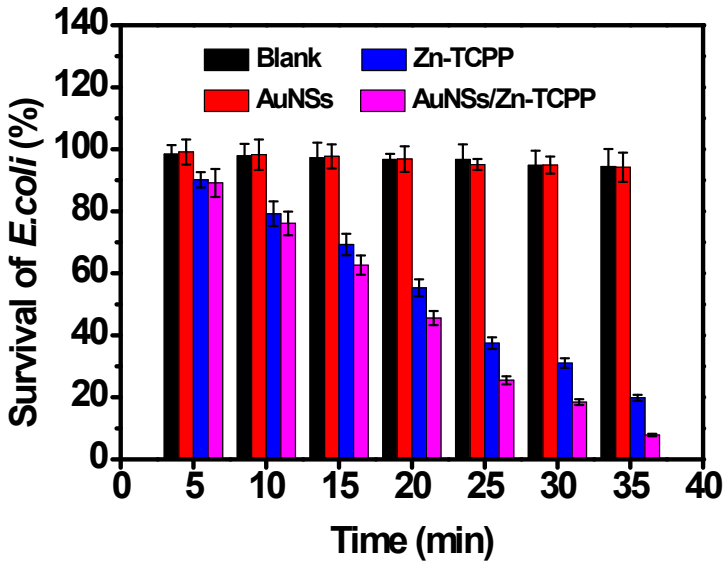

Figure S17. The antibacterial activities of *E. coli* in different groups upon laser irradiation for various times.

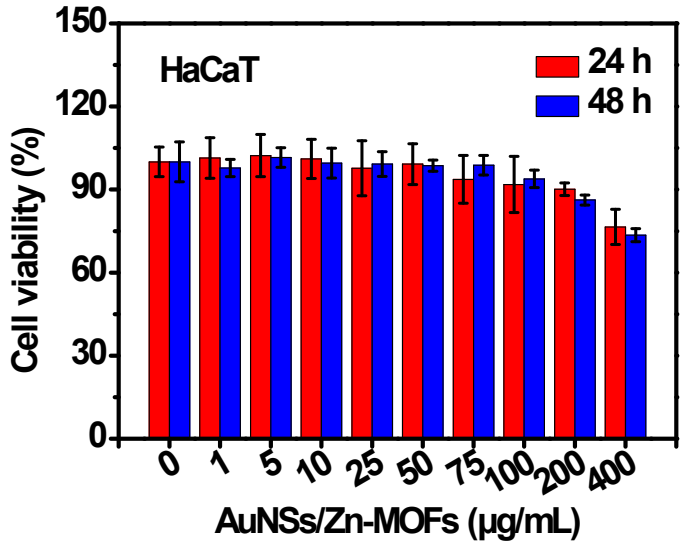

Figure S18. The evaluation of cell (human immortalized keratinocytes, HaCaT) cytotoxicity on AuNSs/Zn-MOFs.

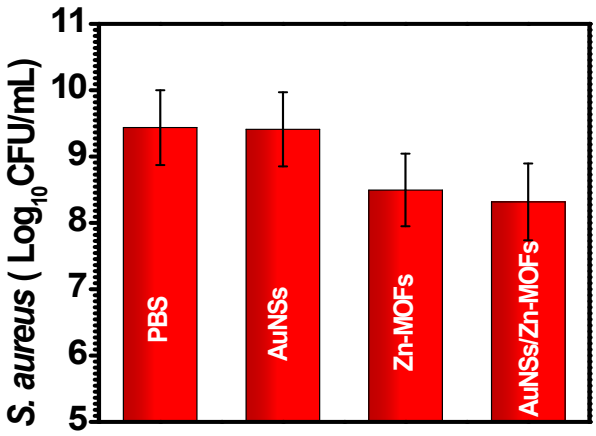

Figure S19. The viability of *S. aureus* after exposed to different groups under light irradiation.

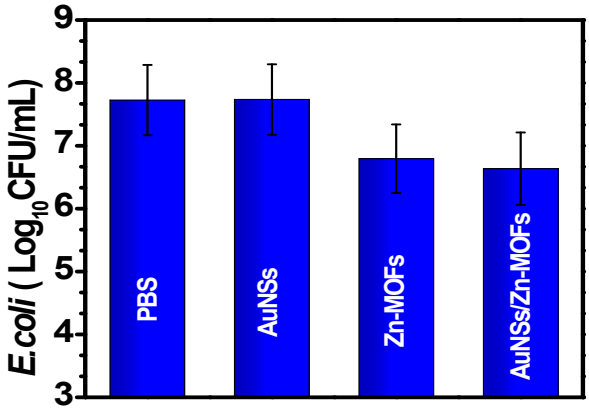

Figure S20. The viability of *E. coli* after exposed to different groups under light irradiation.

Table S1. Comparison of the performance of various method for enhancing ROS generation.

Nanomaterial	Enhancement strategy	Enhancement mechanism	ROS generation enhancement	Reference
PFFBT@HSA	FRET	Extending the phosphorescence lifetime (τ) and strengthening phosphorescence intensity	1.39-fold	(3)
RP/ZnO heterojunction	Charge transfer and electron-hole separation	Reducing the electrons-holes diffuse distance and strengthening the reaction site	~2.22-fold	(4)
GQDs/PCN-224	FRET	GQDs and PCN-224 as a donor-acceptor FRET pair	1.61-fold	(5)
Cu^{2+}-doped PCN-224	Retarding electron-hole recombination	The generated electrons trapped by doped copper	1.11-fold	(6)
Dyad molecule (B-1 and B-2)	RET	Boosting NIR photon utility	1.9-fold	(7)
PMNT/PIC	Changing conformation	Redshifted, new sharp bands in the absorption and fluorescence spectra	~2.38-fold	(8)
PCN-224 nanodots	Decreasing particle size of MOFs	Facilitating the diffusion of generated ROS	2-fold	(9)

TCPO-Ce6	CRET	Electron transfer from TCPO to Ce6 and self-illumination	2.19-fold	(10)
Au NSs/Zn-MOFs	plasmon-induced "dual-excitation effect"	Creating a rich-electron condition and reducing the fermi level due to the LSPR excited hot-electrons injection	2.49-fold	This work

PFFBT: poly{{1,4-(2,5-bis(12′-N,N,N-trimethylammonium)-dodecan-phenylene)-dibromide}-co-(9H-fluorene-2,7-diyl)-co-4,7(2,1,3-benzothiadiazole)}; **HAS:** human serum albumin; **GQDs:** graphene quantum dots; **PMNT:** poly(3-(3'-N,N,N-triethylammonium-1'-propyloxy)-4-methyl-2,5-thiophene chloride); **PIC:** poly-isocyanides; **TCPO:** bis(3,4,6-trichloro2-(pentyloxycarbonyl)phenyl)oxalate; **RP:** red phosphorus; **B-1:** moiety: distyryl-BODIPY; **B-2:** moiety: diiodo-distyryl-BODIPY; **FRET:** fluorescence resonance energy transfer; **RET:** resonance energy transfer; **CRET:** chemiluminescence resonance energy transfer

References

(1) Zhu, W.; Yang, Y.; Jin, Q.; Chao, Y.; Tian, L.; Liu, J.; Dong, Z.; Liu, Z. Two-dimensional metal-organic-framework as a unique theranostic nano-platform for nuclear imaging and chemo-photodynamic cancer therapy. *Nano Res.* **2019,** *12,* 1307-1312.

(2) Kumar, P. S.; Pastoriza-Santos, I.; Rodríguez-González, B.; Abajo, F J. G.; Liz-MarzánKumar, L. M. High-yield synthesis and optical response of gold nanostars. *Nanotechnology* **2008,** 19, 015606.

(3) Guo, L.; Wang, H.; Wang, Y.; Feng, L. Tailor-made polymer nano-assembly with switchable function and amplified anti-tumor therapy. *Adv. Healthc. Mater.* **2020,** *9* (2), 1901492.

(4) Li, J.; Liu, X.; Tan, L.; Liang, Y.; Cui, Z.; Yang, X.; Zhu, S.; Li, Z.; Zheng, Y.; Yeung, K. W. K.; Wang, X.; Wu, S. Light-activated rapid disinfection by accelerated charge transfer in red phosphorus/ZnO heterointerface. *Small Methods* **2019,** *3* (3), 1900048.

(5) Nie, X.; Wu, S.; Mensah, A.; Wang, Q.; Huang, F.; Wei, Q. FRET as a novel strategy to enhance the singlet oxygen generation of porphyrinic MOF decorated self-disinfecting fabrics. *Chem. Eng. J.* **2020,** *395,* 125012.

(6) Han, D.; Han, Y.; Li, J.; Liu, X.; Yeung, K. W. K.; Zheng, Y.; Cui, Z.; Yang, X.; Liang, Y.; Li, Z.; Zhu, S.; Yuan, X.; Feng, X.; Yang, C.; Wu, S. Enhanced photocatalytic activity and photothermal effects of cu-doped metal-organic frameworks for rapid treatment of bacteria-infected wounds. *Appl. Catal. B-Environ.* **2020,** *261,* 11824.

(7) Huang, L.; Li, Z.; Zhao, Y.; Yang, J.; Yang, Y.; Pendharkar, A. I.; Zhang, Y.; Kelmar, S.; Chen, L.; Wu, W.; Zhao, J.; Han, G. Enhancing photodynamic therapy through resonance energy transfer constructed near-infrared photosensitized nanoparticles. *Adv. Mater.* **2017,** *29* (28), 1604789.

(8) Yuan, H.; Zhan, Y.; Rowan, A. E.; Xing, C.; Kouwer, P. H. J. Biomimetic networks with enhanced photodynamic antimicrobial activity from conjugated polythiophene/polyisocyanide hybrid hydrogels. *Angew. Chem. Int. Ed.* **2020,** *59* (7), 2720-2724.

(9) Wang, H.; Yu, D.; Fang, J.; Cao, C.; Liu, Z.; Ren, J.; Qu, X. Renal-clearable porphyrinic metal-organic framework nanodots for enhanced photodynamic therapy. *ACS Nano* **2019,** *13* (8), 9206-9217.

(10) Jeon, J.; You, D. G.; Um, W.; Lee, J.; Kim, C. H.; Shin, S.; Kwon, S.; Park, J. H. Chemiluminescence resonance energy transfer-based nanoparticles for quantum yield-enhanced cancer phototheranostics. *Sci. Adv.* **2020,** *6*, eaaz8400.